This is a postprint of the article published as:
Ren, J., Liu, J., Zhou,S, Kim, M.K. & Song, S. (2022). Experimental study on control strategies of radiant floor cooling system with direct-ground cooling source and displacement ventilation system: A case study in an office building. Energy, 239, art.122410

Experimental study on control strategies of radiant floor cooling system with direct-ground cooling source and displacement ventilation system: A case study in an office building

Jing Ren[1], Jiying Liu[1,2,*], Shiyu Zhou[1], Moon Keun Kim[3], Shoujie Song[1,4]
[1]School of Thermal Engineering, Shandong Jianzhu University, Jinan 250101, China
[2]Built Environment Design and Research Institute, Shandong GRAD Group, Dezhou 253000, China
[3]Department of Civil Engineering and Energy Technology, Oslo Metropolitan University, Oslo, N-0130, Norway
[4]Building Energy Conservation Research Institute, Shandong Antaeus Intelligent and Engineering Co. Ltd, Jinan 250101, China

Corresponding author:
Dr. Jiying Liu, School of Thermal Engineering, Shandong Jianzhu University, #1000 Fengming Road, Jinan 250101, China, Email: jxl83@sdjzu.edu.cn

Abstract
Radiant cooling systems need optimized control strategies to provide superior comfort while maximizing energy-savings. The field measurement method was used to study the operational control of radiant floor cooling (RFC) with a direct-ground cooling source and displacement ventilation (DV) systems. The control methods for the composite system were proposed based on three factors including floor surface temperature relative to the indoor air dew point temperature, the range of indoor/outdoor air temperature and humidity, and the indoor thermal and humidity loads to be countered. These factors were considered in three typical scenarios: intermittent operation, variable initial temperature and humidity conditions, and sudden increases in indoor heat gain, so that maintaining the operative temperature within 26~27°C. The system required that precooling time of the RFC was 2.5~3 times the time to achieve 63% of the temperature change for intermittent operation on weekends, while the DV system was started 1~1.5 h before work time when initial indoor air humidity was higher than 75% and indoor air temperature was higher than 26°C, and supply air flow rate was increased to maximum value under sudden increases in indoor heat gain. The results concluded that dynamic optimal control of the radiant cooling system was achieved.

Keywords: direct-ground cooling source, radiant floor cooling, ventilation, dehumidification, operation control strategies

1 Introduction

Since the 21st century, an increasing amount of attention has been given to energy saving due to emission reduction goals. As such, HVAC technology and radiant cooling/heating air

conditioning systems [1-3], which represent large portions of building energy budgets, have received an especially high amount attention. Many studies and applications have shown that radiant cooling/heating systems can provide improved thermal comfort while being energy efficient [4-6]. High-temperature cooling and low-temperature heating systems use lower-grade cold and heat sources [7-9], this provides favorable conditions for the further promotion and application of radiant terminals. The temperature of the cooling water during summer can be increased from 7°C to 18°C, and the hot water temperature during winter can be reduced to 40°C. Therefore, the system has great energy saving potential [10]. Radiant cooling systems transfer heat between the radiant cooling surfaces and their surroundings via indoor air convective heat transfer and radiative heat transfer. Radiative heat transfer accounts for more than 50% of the total heat transfer in the radiant system [11], increasing the radiative heat transfer with the human body, thus making it central to improving thermal comfort[12]. As a typical radiant system utilizing radiant floor to provide cooling, radiant floor cooling (RFC) systems not only counter solar radiative heat and indoor radiative heat gain in a timely manner, but also reduce the temperature of other internal surfaces and heat gain from the envelope. In an air system, radiative gains are absorbed by the envelope and re-released as convective load, and as a result, the peak cooling rate of a radiant cooling surface is greater than that of an air system [13]. However, the RFC system can only handle the sensible heat load [14]. Condensation will occur when the floor surface temperature is lower than the air dew point temperature without a dehumidification system [15]. Furthermore, the regulation of radiant systems is more complicated than conventional air systems because the response time of the radiant system is significantly longer [16,17]. Given these facts, accurate control strategies are required to meet thermal comfort standards under dynamic weather conditions and indoor heat gain.

Preventing condensation is always a serious concern in radiant cooling systems. Many studies have shown that rates of condensation are higher in the start-up stage, so it is essential to start the ventilation system before (at least one hour earlier) starting the radiant system [18]. Alternatively, the supply water temperature was monitored to be 2–4°C higher than the dew point temperature, depending on predicted thermal load fluctuations [19]. Dehumidification technology is also an effective approach to prevent condensation [20]. Wang et al. [21] applied a liquid desiccant dehumidifier to the radiant cooling system with fresh air supply so as to sufficiently dehumidify the fresh air and reliably regulate the indoor air humidity. Rhee et al. [22] endeavored to avoid local condensation by regulating the temperature of the supply water relative to the highest dew point temperature to improve thermal uniformity of the radiant surface.

The thermal inertia of the radiant terminal can be used by applying an intermittent control strategy [23] combined with controlling supply water temperature and flow rate in radiant panels. These factors can be manipulated to improve response time. Control methods can not only ensure that the indoor thermal and humidity parameters meet comfort standards, but will also reduce energy consumption. Hu et al. [24] found that radiant cooling system conserved cooling energy during unoccupied periods to balance 9–15% of the indoor heat gain during the occupied periods, and the peak sensible cooling loads of the radiant terminal decreased by 32–39% compared with those using conventional scheduling. Thermal energy storage also plays a noteworthy role in building energy efficiency [25,26]. Cho et al. [27] indicated that increasing the heat capacity of the radiant system enabled the rapid absorption of heat through intermittent operation in thermally activated building systems (TABS) with high-thermal inertia to reduce energy consumption. Sui et

al. [28] observed that increasing the start and stop frequency of the pump during a given cooling period increased the cooling capacity of the tube-embedded envelope cooling system. Zhang et al. [29] used the thermal inertia of RFC system to achieve higher energy saving potential via intermittent operation. Lim et al. [30] conducted simulations and experiments on radiant cooling systems which showed that the variable water temperature control in the RFC system enabled a faster response to changes in the indoor thermal environment and had lower energy consumption compared with the variable water flow control system. Tang et al. [31] proposed a novel pulse flow control method that allowed for a 27% reduction of the supply water flow at 50% load operation, and it made the radiant surface temperature distribution more uniform and enabled more accurate control.

Ventilation systems working as supplementary systems enable compound cooling systems to be highly responsive and improve indoor comfort and the operational efficiency [32,33]. Causone et al. [34] examined heat transfer coefficients and concluded that, since the radiant heat transfer coefficient was constant, improving the cooling and heating capacity of the radiant system strongly depended on increasing the convective heat transfer using methods such as increasing the air flow close to the radiant surface. Shan et al. [35] verified that a displacement ventilation (DV) system resulted in a lower draft risk and a 40% higher air change effectiveness in the breathing zone compared to mixing ventilation, and therefore, provided improved thermal comfort and indoor air quality. Tao et al. [36] proposed dynamic control of ventilation to optimize the combination of TABS and ventilation, this led to the lower energy consumption. Michael et al. [37] studied the influence of RFC and DV on the indoor thermal environment, and showed that indoor air quality can still be maintained while reducing the air change rate from 4.5 h^{-1} to 1.5 h^{-1} due to the high air exchange effectiveness of the DV, while the indoor comfort was maintained by regulating the floor temperature. Cui et al. [38] implemented an Airbox convector to form a hybrid radiant panel that enhanced the system's performance even more.

Since the difference between the high temperature chilled water for radiant cooing and natural ambient temperature is usually very small, free cooling can be applied to provide cold energy. The direct-ground cooling system (DGCS), which can provide free cooling source, has attracted a particularly large amount of attention in recent years. In some areas it is feasible to directly provide indoor cooling using only the cooling potential of underground thermal mass. Heat from buried pipes is transferred into the thermal mass of the soil, returning cooled mass to the cooling terminal. When DGCS is combined with a high-temperature radiant terminal, high temperature chilled water can be used to provide indoor cooling [39], significantly reducing energy consumption [40]. Taha et al. [41] studied control methods for DGCS and concluded that the cooling capacity of a cooling terminal was best controlled by regulating the flow of fluid in the ground loop, the intermediate loop, and the building loop. Liu et al. [42] observed that intermittent operation could effectively improve the heat transfer rate of DGCS and alleviated the increase in temperature of the outlet water. Joaquim et al. [43] installed a ground source heat pump to operate only as a ground heat exchanger in the cooling mode to provide free cooling, with only the circulating pump consuming power, demonstrating the energy saving potential of the system along with its ability to shift the peak load.

Indeed, the unique thermal characteristics of RFC systems make the necessary control methods different from those of conventional convective system. It is crucial to know the thermal response of the radiant systems via reliable indicators so as to determine an efficient control

strategy[44], emphasizing the importance of experimental research in the practical applications of RFC systems. However, long-term field studies on the control methods of DGCS with RFC systems based on outdoor weather conditions and indoor load characteristics have been insufficient. Furthermore, most study concentrated on a specific control method covering its application and effect, revealing integrated use of multiple control methods remains to be explored to achieve complementary advantages. It is recommended to implement an earlier start of the ventilation system for dehumidification[1], while condensation on the radiant surface could be effectively prevented when the radiant cooling system was closed during the start-up period[45] . In addition, it has been proved that the control of supply water temperature as a function of outdoor temperature could provide better comfort and energy performance[46]. Besides, ventilation control in the face of indoor heat gain showed high efficiency due to faster responsiveness of ventilation system[14]. Therefore, present study is necessary to combined appropriate control methods to optimize RFC system operation.

In this paper, the field measurement method was used to study the optimal control strategy for a DGCS with RFC system. The experimental room created a real-world scenario in which changes in thermal and humidity parameters in the room were influenced by outdoor weather conditions. The RFC and DV were regulated based on the outdoor weather and indoor loads in an effort to match the cooling capacity of the system with the demand to determine the control optimization potential of the system. The Three experimental scenarios investigated included intermittent operation, variable initial temperature and humidity conditions, and sudden increases in indoor heat gain, which were common and typical conditions having potential to cause the indoor thermal environment to deviate from the comfort range or waste of energy consumption. The effects of corresponding control measures were analyzed in detail to obtain the optimal control strategies for different environmental conditions.

2 Experiment measurement

2.1 Experimental setup

The field test was conducted in a south facing room on the fifth (top) floor of an office building in Jinan with a floor area of 50 m^2. The U-value of the exterior wall was 0.6 W/(m^2·K), that of the roof was 0.55 W/(m^2·K), and that of the external window was 2.4 W/(m^2·K) [47]. Jinan is located in northern China, which is in a cold region as shown in Fig. 1. Fig. 2 shows the outdoor air temperature, relative humidity, and solar radiation in summer during the field study in Jinan. Summer is hot and rainy and lasts for 105~120 days, there was a low frequency of temperatures above 35°C. Therefore, DGCS may have a good advantage and can be applied to the office building to counter a certain level of indoor heat gains in summer.

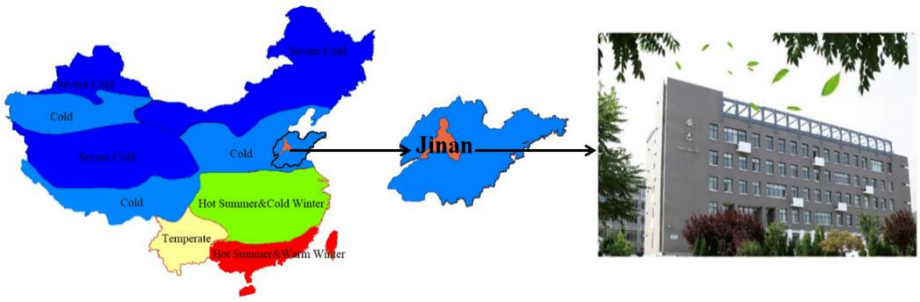

Fig. 1 The climate location of Jinan and an outdoor view of the office building.

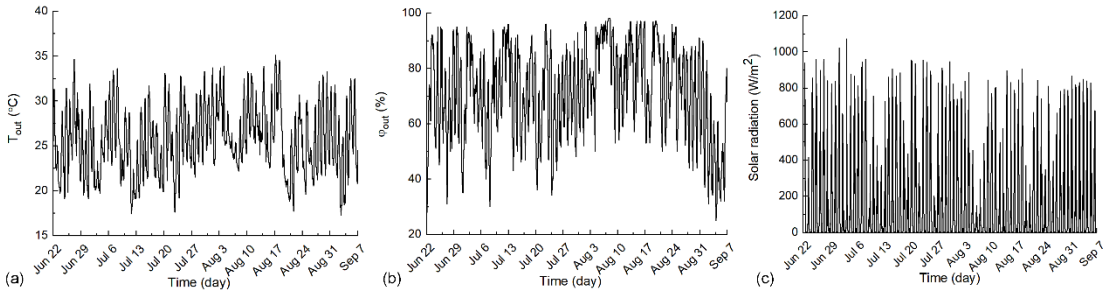

Fig. 2 Weather conditions during the field study in summer, (a) outdoor air temperature (T_{out}), (b) outdoor air relative humidity (φ_{out}), and (c) solar radiation.

The integrated DGCS with RFC and DV system is depicted in Fig. 3. The cooling energy supplied to the radiant floor terminal comes entirely from the ground heat exchanger in summer. Therefore, the underground pipe water was directly supplied to the room without passing through the heat pump unit. Meanwhile, an air supply was used to ventilate the room after passing through the air handling unit. The chilled water of the DV system is generated by the heat pump unit during the off-peak power period at night, conserved in the chilled water storage tank to provide cooling energy for the air handling unit, and used to remove the air supply heat and humidity loads during the working period.

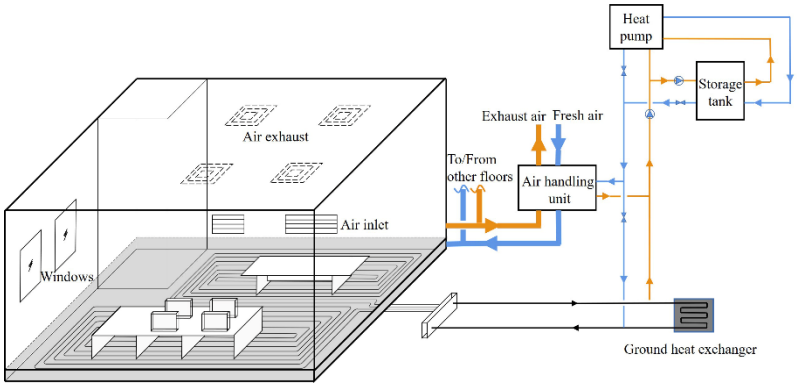

Fig. 3 Schematic diagram of the DGCS with RFC and DV systems.

Fig. 4 The field test environment in the office room.

The field test environment is shown in Fig. 4. The measurement parameters included supply and return water temperatures and flow rates, floor surface temperature, wall and ceiling temperatures, room air temperature and humidity, black globe temperature, CO_2 concentration,

and ventilation air flow rate. The layout of measuring points is shown in Fig. 5. The floor surface temperature measuring points were placed near walls to the east, west, north, and south of the room. The wall temperature measuring points were centered on their respective walls, and ceiling measuring points were uniformly distributed on the ceiling. Two CO_2 testers were placed at vertical heights of 1.1 m in the center of the room and at the supply air inlets. One indoor air parameter measuring point was placed at the vertical height of 1.1 m in the center of the room, and the other six measuring points at vertical heights of 0.1 m were uniformly distributed in the room. Two black globe temperature measuring points were placed at vertical heights of 1.1 m in the center of the room and near the south (exterior) wall. The ventilation air measuring points were placed at the supply air inlets. The supply and return water temperature measuring points were placed at manifolds on the supply and return water pipes. The detailed parameters of experimental equipment are shown in Table 1.

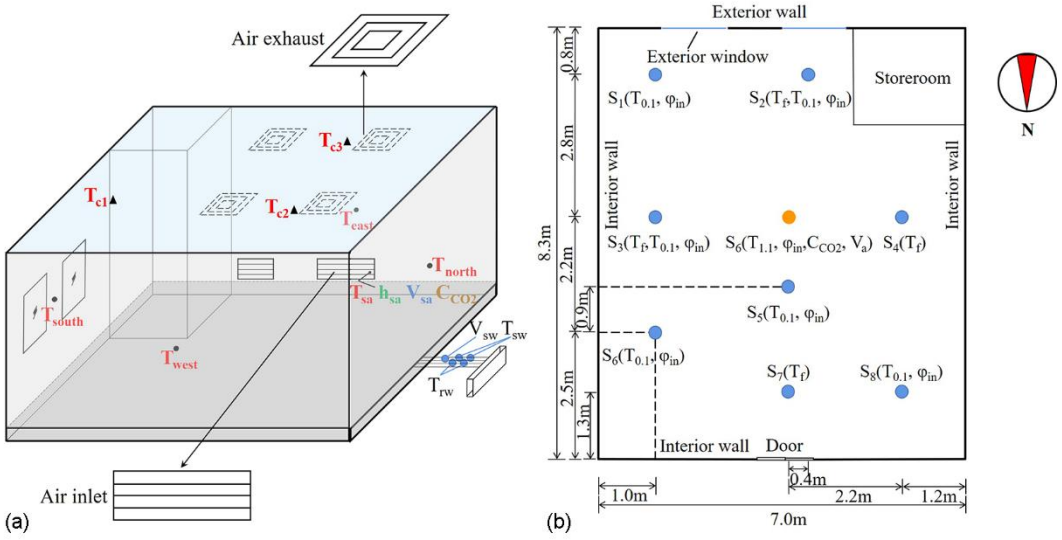

Fig. 5 Layout of measuring points, (a) full view of the experimental office, and (b) top view of measuring points.

Table 1 Summary of the experimental instruments.

Parameters	Instruments	Range	Accuracy	Manufactory and country
Room air temperature	Temperature and humidity meter	-20~80°C	±0.5°C	Beijing Jantytech, China
Room air relative humidity	Temperature and humidity meter	0~100%	±3%	Beijing Jantytech, China
Floor surface temperature	K-type thermometer (surface mount type)	-50~100°C	±0.5°C	Shenzhen CEM, China
Wall and ceiling temperature	K-type thermometer (surface mount type)	-50~100°C	±0.5°C	Shenzhen CEM, China
Black globe temperature	Black globe temperature meter	-20~70°C	±0.3°C	SWEMA, Sweden
Ventilation air temperature	Air multi-parameter (temperature, humidity and velocity) meter	-10~60°C	±0.3°C	TSI, USA
Ventilation air relative humidity	Air multi-parameter (temperature, humidity and velocity) meter	5~95%	±3%	TSI, USA

Ventilation air flow rate	Air multi-parameter (temperature, humidity and velocity) meter	0~30 m/s	±0.015 m/s	TSI, USA
Water temperature	K-type thermometer	-50~100°C	±0.5°C	Shenzhen CEM, China
Water flow rate	Water flow meter	1.2~12 m^3/h	±1%	Hangzhou Sinomeasure, China
CO_2 concentration	CO_2 meter	0~6000 ppm	±3%	Taiwan TES, China

2.2 Experimental schemes

The basic control method of composite system included two stages control for different indoor loads handling requirements (Fig. 6). One is activation control before work time. It is required to determine sufficient precooling time ($\tau_{precooling}$) of RFC to deal with the heat accumulated after being shut down over unoccupied time, which is concerned with thermal response of RFC generally described by the τ_{63} value for the cooling process of the radiant surface. τ_{63} is the time taken to achieve 63% of the desired temperature change [48]. Meanwhile, preventing condensation should be paid much attention to, which required floor surface temperature (T_f) 2°C higher than air dew point temperature (T_{dp}) near the floor surface. Moreover, a large amount of indoor humidity loads should be removed via determining DV pre-dehumidification time and supply air flow rate (V_{sa}) based on initial indoor humidity (φ_{in}) before activating DV and target indoor humidity at start time of work.

The other is operational parameters regulation during operation. It aims to handle heat load caused by outdoor and indoor heat gain. On the one hand, supply water temperature (T_{sw}) control of RFC correlated to outdoor air temperature (T_{out}) along with supply water flow rate (V_{sw}) control are used in response to dynamic change of outdoor weather. On the other hand, when indoor heat gains (ΔQ) suddenly increase, DV regulation of supply air temperature (T_{sa}) and supply air flow rate should be made to remove increasing heat and humidity load.

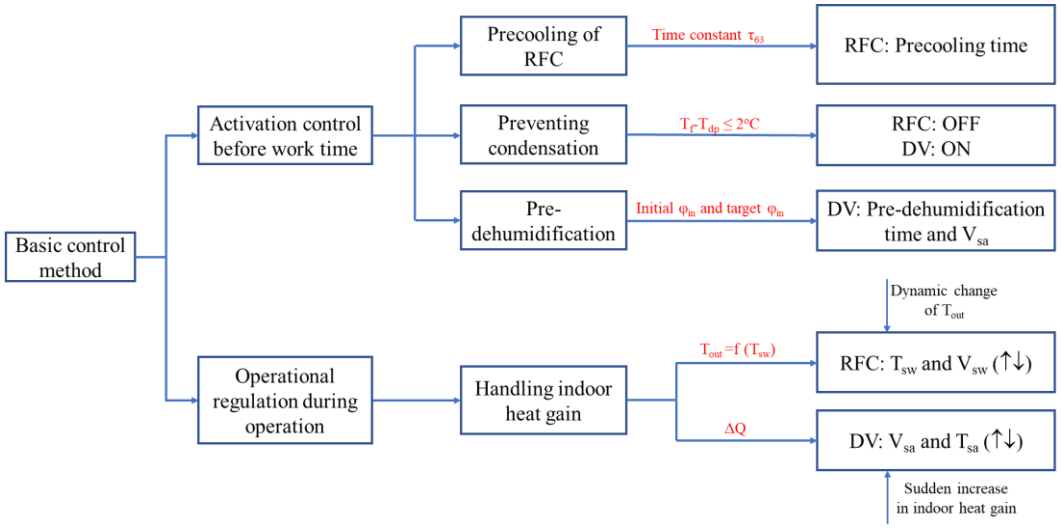

(a)

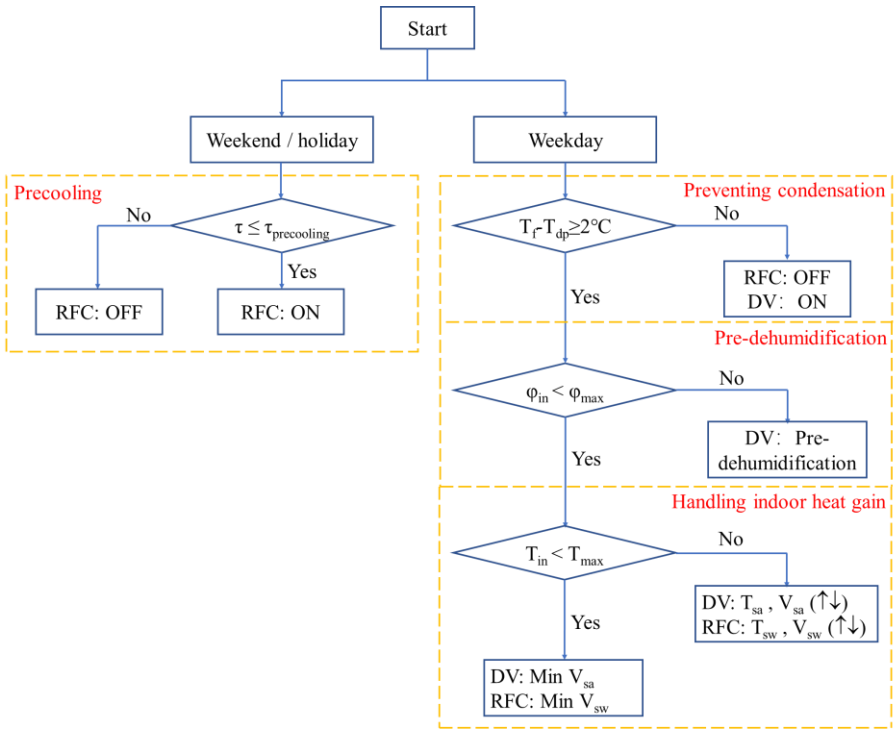

(b)

Fig. 6 Basic control method of composite system, (a) Control concept, (b) Control logic (τ is the time from current time to start time of work, φ_{max} is upper indoor air humidity limit, and T_{max} is upper indoor air temperature limit).

Precooling time of RFC in this study is first determined based on fact that the response time τ_{95} equals three times τ_{63}, as indicated by Lienhard [49]. Moreover, considering the realistic operation conditions in this experiment, precooling time for the RFC system was finally set as 2.5~3 times τ_{63}. As for DV system control for pre-dehumidification, the air humidity (75%) verified in Appendix A is taken as key point to determine start-up time and supply air flow rate of DV system.

To counter indoor heat load originated from outdoor and indoor heat gain, specific parameters are defined to determine regulation to be implemented. According to the relationship between supply water temperature and outdoor air temperature proposed by Song [50], the key point of outdoor air temperature at which the operational parameters of DV and RFC system need to be adjusted was determined to be 32°C. Since the radiant heat transfer coefficient remains essentially constant within the indoor air temperature range, and the more important factor is that the supply water temperature of the RFC system is maintained relatively constant due to the usage of direct-ground cooling source [51]. Therefore, it is critical to control the DV system so as to adjust the cooling capacity in response to changes of indoor heat gains over time [52]. Based on the above control concept and principle, along with consideration of dynamic change of thermal environment and operational performance of the composite system, the control strategies were put forward. The detailed explanation of control strategies especially for precooling time along with the key points of adjusting dehumidification operation and the cooling capacity of the composite system can be found in the Appendix A. Fig. 7 illustrates the control strategy for the RFC and DV system.

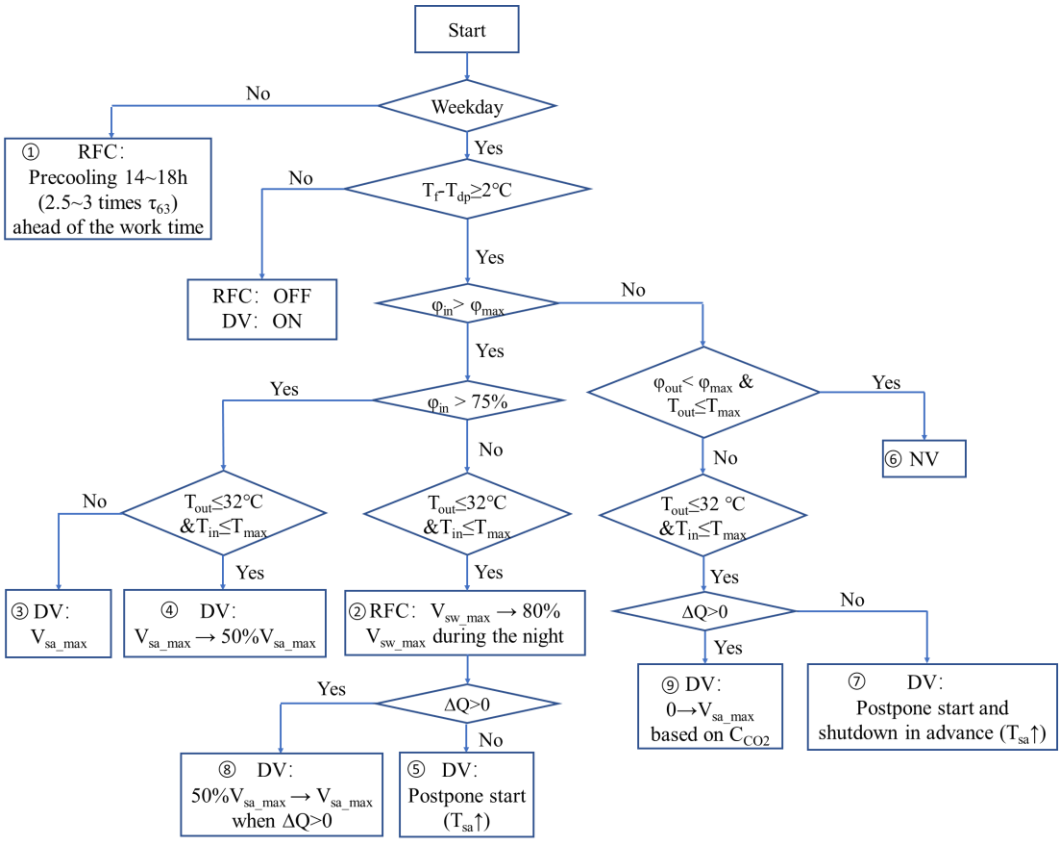

Fig. 7 Proposed experimental control strategies in this experimental case.

A radiant floor system, as a kind of thermally activated system, can take advantage of thermal performance of radiant floor through intermittent operation control in the summer [53]. This study considered two primary approaches for intermittent operational control of the RFC system.

(1) Intermittent operation on weekends

The RFC system is shut down on weekends and initiated again ahead of weekdays. As mentioned before, $\tau_{precooling}$ for the RFC system is 2.5~3 times τ_{63}, and accordingly the maximum temperature decrease during $\tau_{precooling}$ in the present experiment, which is the floor surface temperature difference at the initial stage and stable stage, was close to 2°C. Therefore, it is required to activate the RFC system when the increase of T_f reached 2°C, resulting in acceptable thermal comfort condition during the working period.

(2) Intermittent operation during weekday nights

The supply water flow rate of the RFC system at night is reduced to 80% of that during the working period on weekdays. The decrease of the supply water flow rate is determined based on the indoor cooling requirement.

The operational control of the DV system under different outdoor weather conditions and indoor heat/humidity load conditions can be divided into the following three scenarios.

(1) High initial air humidity in the room (φ_{in} > 75%)

The DV system is initiated 1~1.5 h ahead of the working time (9:00), which is adjusted according to the latent heat load to be removed and dehumidification rate. After removing the start-up humidity load, the supply air flow rate is regulated to change the heat removal rate of the DV system in response to the indoor heat gain affected by outdoor air temperature conditions, which was characterized by the relationship between T_{out} and 32°C as illustrated in Appendix A.

(2) Low initial air humidity in the room (φ_{in} < 75%)

The DV system is initiated if the indoor humidity condition reaches φ_{max} or at the high temperature at noon, along with the increase of supply air temperature by 1~2°C at the initial time when $T_{out} \leq 32$°C in the daytime. This control principle only starts the DV system when the RFC system cannot handle the indoor heat and humidity loads, and the supply air temperature can be properly increased at the initial time to balance the relatively lower heat gain. Furthermore, natural ventilation (NV) replaces the DV system to supply fresh air when $T_{out} \leq 28$°C and $\varphi_{out} \leq 70\%$.

(3) Sudden increase of indoor heat gain

This study also addressed cases when the ΔQ_{sen} equals 344 W and ΔQ_{lat} equals 146 W. The DV system uses V_{sa_max} to handle the increased indoor heat gain and CO_2 concentration (Cco_2), and then the supply air flow rate can be regulated based on the changes of indoor thermal environment parameters.

Table 2 lists descriptions of various working conditions and the corresponding control measures, and the specific processes are illustrated in Fig. 8.

Table 2 Case descriptions and control strategies.

Case	Date	Initial indoor condition	RFC or ventilation
1*	Aug. 16 Aug. 23	$T_f \geq 26$°C, $T_{in} > 26$°C	RFC ON: 17:00, V_{sw}: V_{sw_max} RFC ON: 13:00, V_{sw}: V_{sw_max}
2*	Sep. 8	$T_f \leq 24$°C, $T_{in} < 26$°C	RFC V_{sw}: $V_{sw\_max} \rightarrow 80\%\ V_{sw\_max}$ after 17:00
3	Aug. 18	$\varphi_{in} > 80\%$, $T_{in} \geq 26$°C	DV ON: 1.5 h before work time (9:00); V_{sa}: V_{sa_max}
4	Aug. 31	75% < φ_{in} < 80%, T_{in} < 26°C	DV ON: 1 h before work time (9:00); V_{sa}: $V_{sa\_max} \rightarrow 50\%\ V_{sa\_max}$; 2 h after start time
5	Sep. 1	70% < φ_{in} < 75%, T_{in} < 26°C	DV ON: After work time (9:00) T_{sa}: Increment by 1~2°C
6	Sep. 3**	$\varphi_{in} < 65\%$, $T_{in} < 26$°C	NV, Open windows when φ_{in} and C_{CO2} reach high levels
7	Sep. 8	$\varphi_{in} < 65\%$, $T_{in} < 26$°C	DV ON: 12:00 when $T_{out} \geq 30$°C T_{sa}: Increment by1~2°C OFF: 16:00 when T_{in} remains stable
8	Aug. 27	70% < φ_{in} < 75%, T_{in} < 26°C; $Q \uparrow$, ΔQ_{sen} = 344 W, ΔQ_{lat} = 146 W	DV V_{sa}: 50% $V_{sa\_max} \rightarrow V_{sa\_max}$ when $Q \uparrow$ $V_{sa\_max} \rightarrow 50\%\ V_{sa\_max}$ half hour after $Q \downarrow$
9	Sep. 2	65% < φ_{in} < 70%, T_{in} < 26°C; $Q \uparrow$, ΔQ_{sen} = 344 W, ΔQ_{lat} = 146 W	DV V_{sa}: $0 \rightarrow V_{sa\_max}$ when C_{CO2} increases to 700 ppm, regulation based on C_{CO2} during operation

*Note: Intermittent operation cases.

**Note: Outdoor air conditions on Sep. 3: $T_{out} \leq 28$°C and $\varphi_{out} \leq 70\%$.

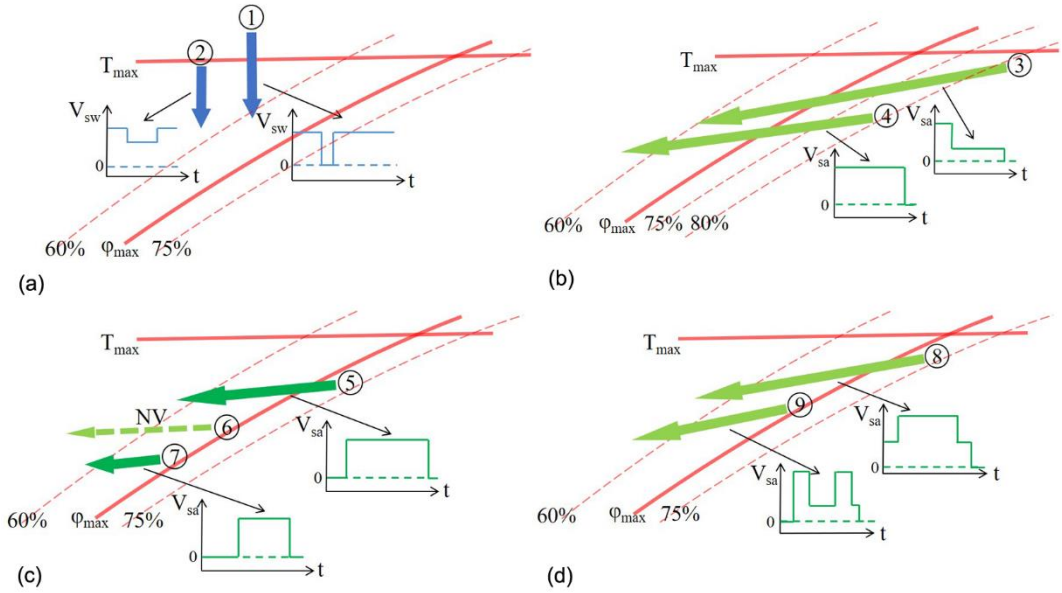

Fig. 8 Air handling processes, (a) case 1~2, (b) case 3~4, (c) case 5~7, and (d) case 8~9.

2.3 Experimental evaluation index

2.3.1 Radiant uniformity coefficient

The radiant uniformity coefficient (S) [48] was used to reveal the cooling capacity of the radiant floor in this paper. A lower uniformity coefficient means that the difference between the average temperature and the minimum temperature of the radiant floor is small. Therefore, the RFC system will have greater cooling capacity with better uniformity of the radiant surface temperature. The calculation method is described by Eq. (1):

$$S = \frac{T_{s,max} - T_{s,min}}{T_g - T_h} \quad (1)$$

where, $T_{s,max}$ and $T_{s,min}$ are the maximum and minimum temperatures of the radiant panel surface, respectively; and T_g and T_h are the radiant panel supply and return water temperatures, respectively.

2.3.2 Operative temperature

The heat exchange between the radiant floor surface and the indoor thermal environment occurs mainly via radiative and convective heat transfer. Therefore, the operative temperature (T_{op}), which combines the indoor air temperature and mean radiant temperature, can be used as the evaluation index for indoor thermal comfort (see Eq. (2)). The mean radiant temperature (T_{mrt}) was calculated using the black globe thermometer measurements (see Eq. (3)). Additionally, the indoor air velocity was less than 0.2 m/s and the difference between the mean radiant temperature and indoor air temperature was less than 4°C, which simplified the calculation of T_{op} to Eq. (4)[48].

$$T_{op} = \frac{h_c T_a + h_r T_{mrt}}{h_c + h_r} \quad (2)$$

$$T_{mrt} = [(T_g + 273.15)^4 + \frac{1.1\times10^8 v_a^{0.6}}{\varepsilon D^{0.4}} \times (T_g - T_a)]^{0.25} - 273.15 \quad (3)$$

$$T_{op} \approx T_{adjust} = \frac{T_a + T_{mrt}}{2} \quad (4)$$

where, T_g is black globe temperature, T_a is air temperature, h_c is convective heat transfer coefficient, and h_r is radiative heat transfer coefficient.

3 Results and discussion

3.1 Indoor comfort

The indoor T_{op} was generally maintained within 26~27°C during the experiment. The T_{op} during the typical cases are shown in Table 3, all of which met ASHRAE thermal comfort standards [54] (25°C ≤ T_{op} ≤ 28°C).

Table 3 T_{op} (°C) of typical cases during the working period (9:00–17:00).

Case	Date	Maximum	Minimum	Average	Standard deviation
1	Aug. 17	26.4	25.5	26	0.19
	Aug. 24	25.8	24.8	25.3	0.1
2, 7	Sep. 8	27.1	25.9	26.6	0.09
3	Aug. 18	27.1	25.6	26.6	0.23
4	Aug. 31	26.9	25.5	26.4	0.28
5	Sep. 1	26.8	25.8	26.4	0.15
6	Sep. 3	27	25.4	26.3	0.09
8	Aug. 27	25.9	24.6	25.3	0.14
9	Sep. 2	27.2	25.7	26.7	0.14

3.2 Cases of intermittent operation

3.2.1 Intermittent operation on weekends

τ_{63} of the RFC system is the time it takes T_f to reach 63.2% of the total variability range. It can be seen from Fig. 9 that τ_{63} is used to reflect the rate of radiant terminal's change from start-up to stable heat transfer. The decay process of floor temperature can also be seen, as Fig. 9(a) and (b) show the changes in T_f after the initiation of the RFC system. When the floor water supply system began operation on Aug. 16, T_f was 26.5°C. T_f reached 63% of the total variability range after 5.4 h, and then gradually decreased to be relatively stable at 24.2°C once the floor water supply system had been operating for 13.9 h. During daytime on Aug. 17, T_f surpassed 24°C, with a peak temperature close to 24.5°C. On Aug. 23, when the floor water supply system began operation, the initial T_f was 25.7°C, it reached 24°C after 5.8 h, then continuously decreased and gradually stabilized at 23.6°C approximately 17.6 h after start-up. Nevertheless, T_f was lower than 24°C during the daytime on Aug. 24. The difference between τ_{63} of the RFC system on Aug. 16 and Aug. 23 was 24 minutes, which indicated that the thermal response of the radiant terminal was affected by the indoor thermal environment during the start-up stage and continued operation. The heat transfer rate of the radiant terminal decreased, leading to a slowdown in the temperature decrease after τ_{63}. Therefore, τ_{63} accounted for less than 1/2 of the total T_f variability range.

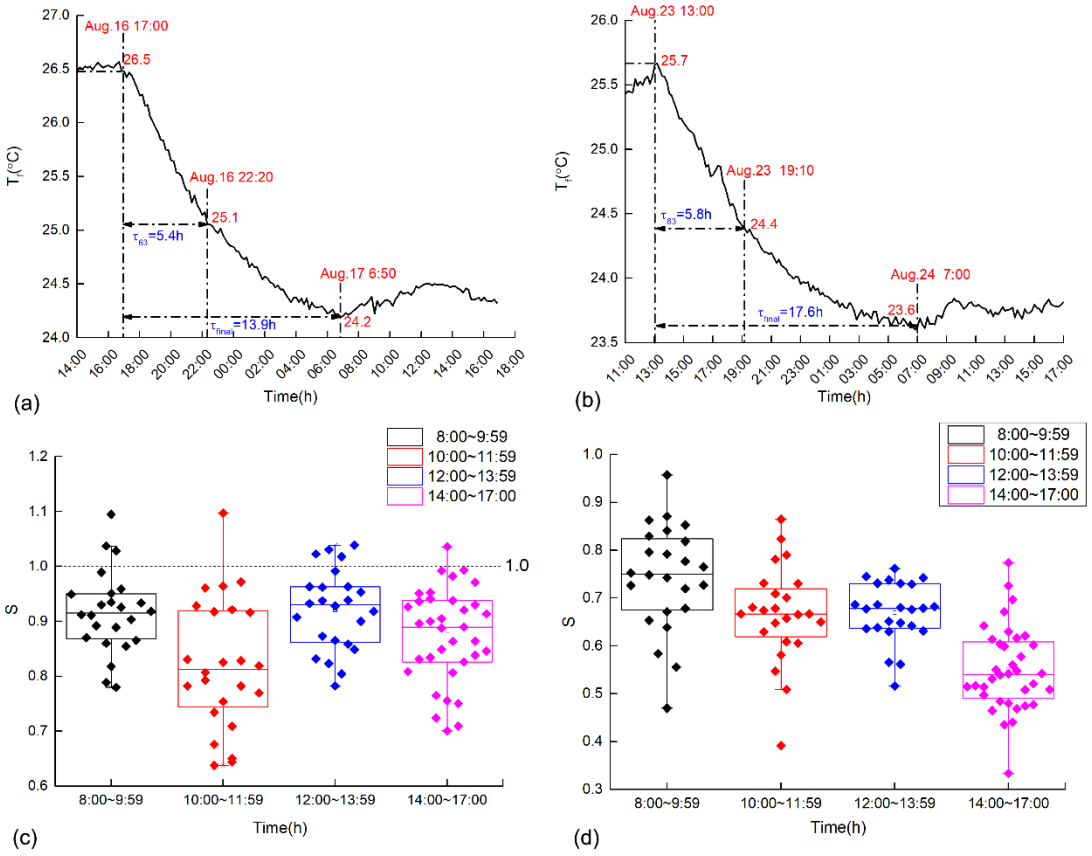

Fig. 9 The decay process of floor temperature, (a) T_f change on Aug. 16–17, (b) T_f change on Aug. 23–24, (c) S range for 4 periods on Aug. 18, and (d) S range for 4 periods on Aug. 24.

When the floor water supply system was activated, T_f was higher on Aug. 16 than on Aug. 23. Specifically, the floor water supply system was activated in the afternoon on Aug. 16 when T_{out} decreased to a low level, while the floor water supply system was activated at noon on Aug. 23 when T_{out} was higher. As a result, the T_f gradient on Aug. 17 was slightly larger than that on Aug. 23. Since the temperature gradient between the floor surface and the chilled water was smaller on Aug. 23, the total decrease in T_f on Aug. 23 was 0.3°C smaller than that on Aug. 17. However, after stabilizing, the temperature on Aug. 24 was lower than that on Aug. 17, despite the similar time of T_f change. In addition, comparing the S ranges for the 4 periods on these two days (Fig. 9 (c), (d)), the uniformity of the T_f distribution was better on Aug. 24. It could be concluded that using a more advanced start-up time when the initial floor temperature is lower will increase the duration of the cooling time of the RFC system without a great fluctuation in T_{out}. Based on the performance of the RFC system and the indoor thermal environment, the actual duration for the whole cooling process equals 2.5~3 times τ_{63} along with the difference between initial T_f and stable T_f close to 2°C, which enabled T_f to return to designed level on workdays with good uniformity and ensured the cooling capacity of the radiant floor system is sufficient.

3.2.2 Intermittent operation at night on weekdays

The changes of T_f and T_{in} under a low flow rate operation of the RFC system during the comparable outdoor weather conditions on Sep. 9 and Sep. 8 are shown in Fig. 10. The T_f of low flow rate (80%V_{sw_max}) operation at night was similar to that of the constant flow rate (V_{sw_max}) operation. Besides there was high similarity between T_{in} on Sep. 9 and Sep. 8, with a difference smaller than 0.5°C. It was notable that, with the DV system closed, when the heat gain of the room

was small due to the low T_{out} at night, the supply water flow rate of the radiant floor system at night could be reduced to 80% based on the cooling capacity of the RFC system. The cooling energy provided by the chilled water was sufficient to support the heat exchange between the floor surface and the indoor air and other internal surfaces without allowing heat storage in the floor and keeping T_f relatively stable. Moreover, the cooling capacity of the radiant floor cooing system must be maintained to cope with increased T_{out} and indoor heat gains, so as to keep T_{in} within the allowable comfort range while also reducing energy consumption.

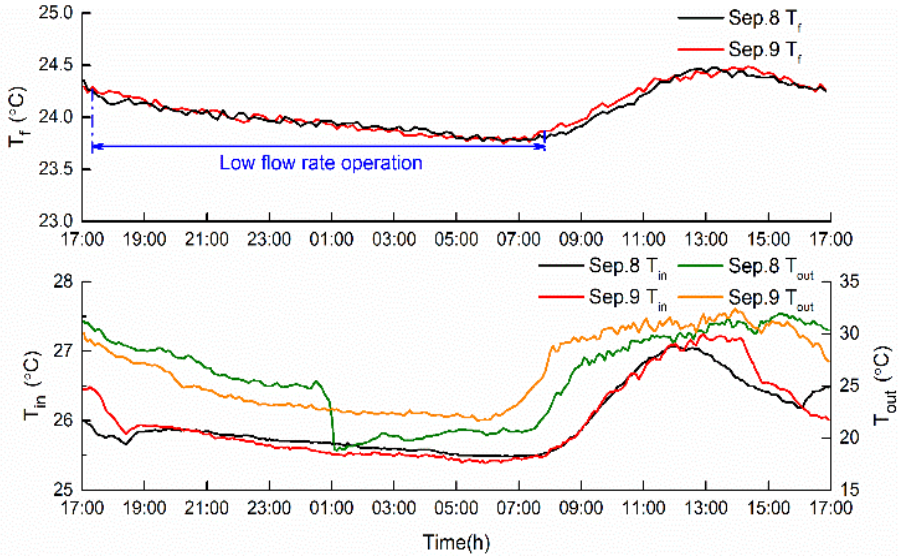

Fig. 10 The changes of T_f and T_{in} under low flow rate operation of the RFC system.

3.3 Cases with different initial indoor temperatures and humidities

3.3.1 Initial conditions: high humidity and high temperature

Fig. 11 shows the φ_{in} reduction process with different start-up times for the DV system. φ_{in} was higher than 80% when the DV system was activated on Aug. 18. The dehumidification time was determined based on the target relative humidity at work time and the dehumidification rate of the DV. The actual pre dehumidification amount was 3.8 g/kg before work time. While the advanced start-up time of the DV system on Aug. 24 was unable to sufficiently dehumidify the indoor start-up humidity load, which resulted in φ_{in} being above 70% at 9:00. During the working period on Aug. 18 and Aug. 24, φ_{in} tended to stabilize as the dehumidification capacity of the DV system reached an equilibrium with the indoor humidity gain. But φ_{in} was higher on Aug. 24 due to the insufficient dehumidification during the start-up stage. Therefore, it is necessary to extend the start-up time of the DV system when the indoor environmental humidity is particularly high to make sure φ_{in} is within the allowable range by the working period.

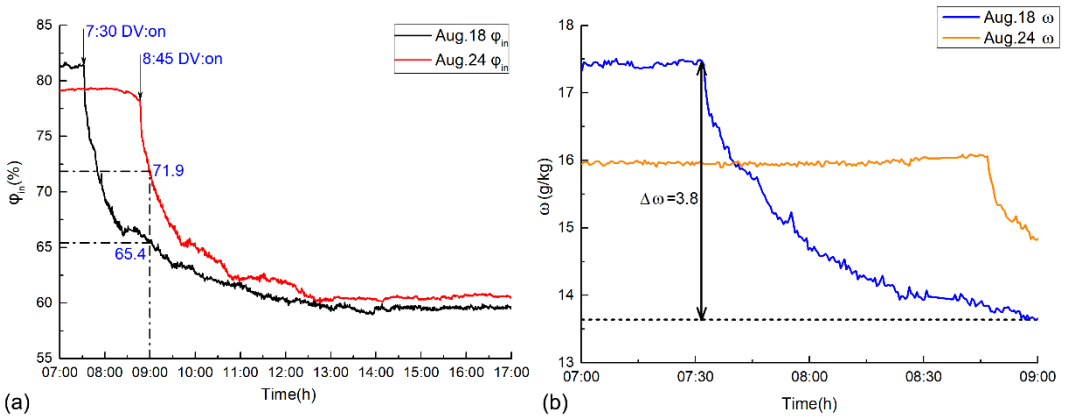

Fig. 11 φ_{in} reduction process under different start-up times of the DV system, (a) φ_{in} change over the whole day, and (b) ω change in the start-up stage.

3.3.2 Initial conditions: high humidity and low temperature

High humidity and low temperature case (1): Fig. 12 depicts the changes of T_{in}, φ_{in}, and C_{CO2} when V_{sa} was held constant or when it varied. On Aug. 18, since the DV system was started at V_{sa_max}, φ_{in} decreased to 65% by the work time, finally stabilizing at 60% with minor fluctuations while the T_{in} was maintained below 26.8°C. The indoor C_{CO2} increased significantly with an increase in number of occupants, but gradually stabilized at less than 900 ppm due to the supply air. However, when the supply air flow rate of V_{sa_max} was restricted to 50% V_{sa_max} during the working period on Aug. 31, φ_{in} was still within 55%~60%, and T_{in} was below 26.5°C with no obvious fluctuation. The indoor C_{CO2} increased significantly over a short period, but remained basically stable below 800 ppm after some time. It could be concluded that when the indoor environment had high humidity and a low temperature, it is important to start the DV system at V_{sa_max} to achieve the required dehumidification before reducing it to 50% V_{sa_max}, which is sufficient to counter changes in the indoor thermal and humidity loads and ensure the indoor air quality.

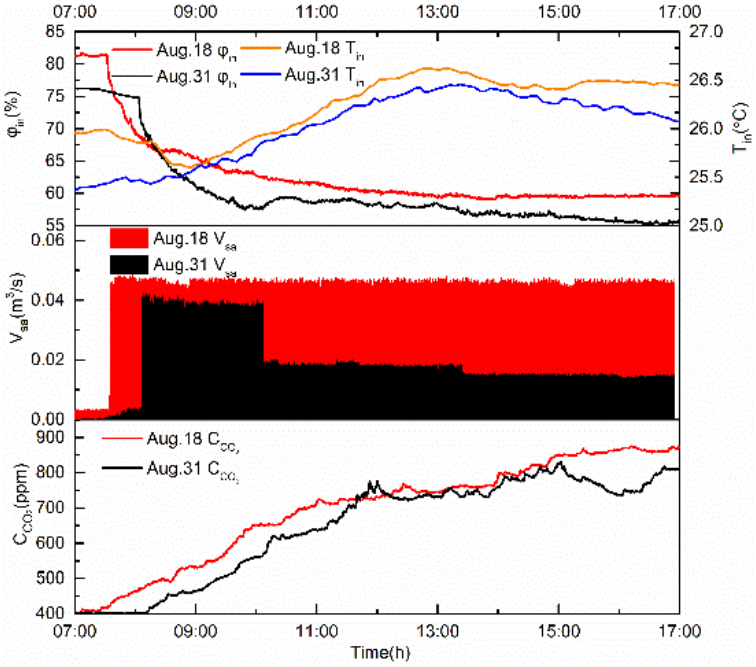

Fig. 12 The changes of T_{in}, φ_{in}, and C_{CO2} under constant V_{sa} control and variable V_{sa} control.

High humidity and low temperature case (2): Fig. 13 shows how T_{in}, φ_{in}, and C_{CO2} changed when DV start-up time was postponed and T_{sa} was increased, compared with no air supply. φ_{in} on Aug. 29 remained at about 70% with no air supply, and the indoor C_{CO2} continuously increased and exceeded 800 ppm. φ_{in} on Sep. 1 decreased slightly before the DV system was activated, but when the DV system began operation with T_{sa} increasing by 1~2°C, the indoor residual heat and humidity were removed. φ_{in} decreased to 55%, while the increase in the indoor C_{CO2} slowed, it stabilized at approximately 700 ppm. This indicated that the start-up time of the DV system can be properly postponed combined with an increase of T_{sa} when the indoor environment has a high humidity and low temperature. Furthermore, the decreased cooling capacity of the DV system was still sufficient to counteract the indoor humidity load and the sensible heat gain, and therefore T_{in} and φ_{in} were controlled within the allowable range.

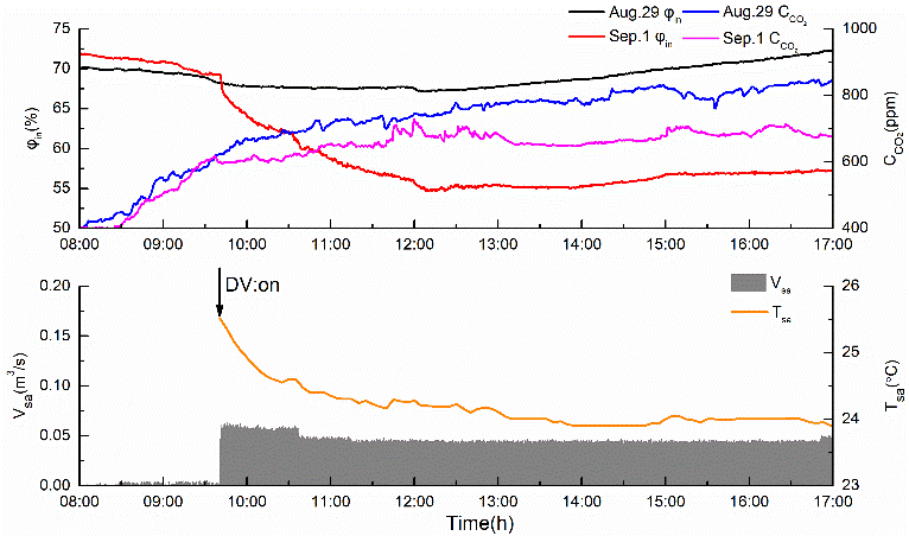

Fig. 13 The changes of T_{in}, φ_{in}, and C_{CO2} when DV start-up time was postponed and T_{sa} was increased, compared with no air supply.

3.3.3 Initial conditions: low humidity and low temperature

Low temperature and low humidity case (1): Fig. 14 illustrates the changes of T_{in}, φ_{in}, and C_{CO2} when supplemented with NV without DV. T_{in} was generally below 27°C during the working period on Sep. 3. φ_{in} and C_{CO2} increased gradually, and windows were opened for NV when C_{CO2} reached 900 ppm. φ_{in} and C_{CO2} rapidly decreased to low levels and remained stable with the influx of fresh air. This demonstrated that NV can be used to remove the indoor humidity load, improve indoor air quality, and save energy when T_{out} and φ_{out} are both suitable for ventilation.

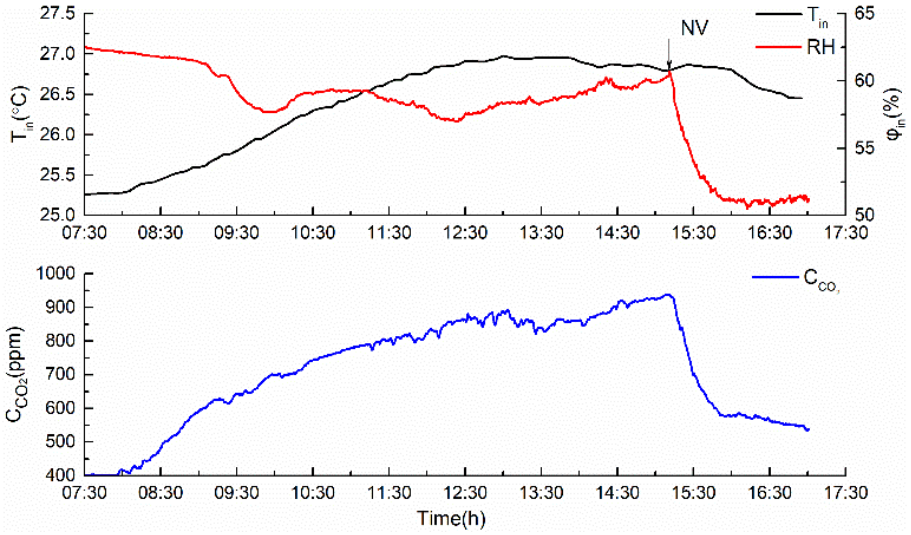

Fig. 14 The changes of T_{in}, φ_{in}, and C_{CO2} when supplemented with NV without DV.

Low temperature and low humidity case (2): Due to the differences in indoor heat gain between Aug. 18 and Sep. 8, the latter had a shorter DV operation time system and higher T_{sa}, and the effect on T_{in} and φ_{in} is illustrated in Fig. 15. On Aug. 18, the DV system was started in the morning, and it continued operation with lower T_{sa} until 17:00 to ensure suitable T_{in} and φ_{in} were maintained. On Sep. 8 however, due to the lower initial T_{in} and φ_{in} and less heat being transferred to the room, the DV system was started during the peak temperature at noon to provide supplementary cooling and dehumidification. This resulted in T_{in} beginning to decrease and φ_{in} rapidly decreasing. The DV system was shut down in advance of the end of working period as T_{out} decreased in the afternoon, and then T_n and φ_{in} underwent a slight increase and gradually stabilized. Therefore, it could be concluded that it is acceptable to shorten the operational time of the DV system and increase T_{sa} when the indoor environment has low temperature and low humidity, achieving better thermal comfort and energy saving.

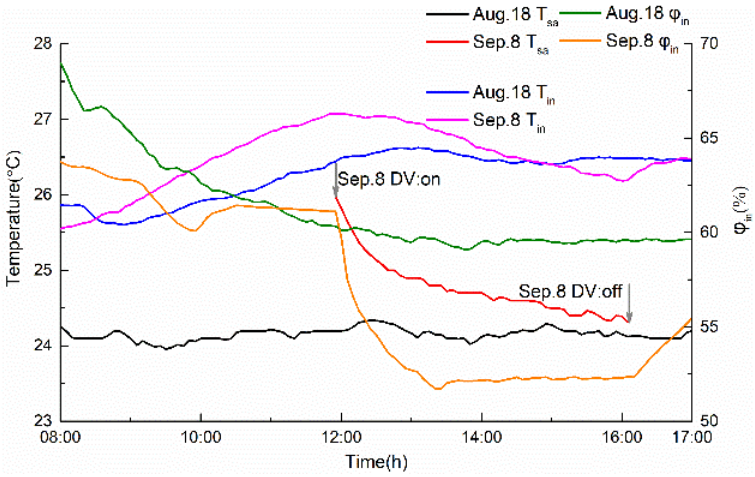

Fig. 15 The changes of T_{in} and φ_{in} under shortened DV system operating time and higher T_{sa}.

3.4 Cases of sudden increase in indoor heat gains

3.4.1 Responses based on the number of occupants

The changes of T_{in}, φ_{in}, and C_{CO2} when V_{sa} is regulated based on the number of occupants are shown in Fig. 16. Due to the relatively high initial φ_{in} on Aug. 27, the DV system was started at 50% V_{sa_max} for dehumidification so that φ_{in} decreased to below 70%. The supply air flow rate in the

room was increased with increasing indoor heat gain (ΔQ_{sen} = 344 W, ΔQ_{lat} = 146 W) to strengthen the convective heat transfer and improve the cooling capacity. Thus, the increased thermal and humidity loads in the room were counteracted and indoor comfort was maintained. The change of C_{CO2} became stable after a small increase, and the decreasing gradient of φ_{in} gradually lessened until stabilizing. T_{in} fluctuated with the changes in heat transfer from outside coinciding with outdoor temperature change, and was kept below 26°C with high-flow rate operation. After the number of occupants decreased, the supply air flow rate was maintained for half an hour at V_{sa_max} to remove the residual heat and humidity, after which it was decreased to 50% V_{sa_max}, resulting in small fluctuations in T_{in}, φ_{in}, and C_{CO2} before they quickly stabilized. This indicated that the increase of supply air flow rate in response to a sudden increase in indoor heat load is a quick way to supplement the cooling capacity and avoid large fluctuations of T_{in} and φ_{in} and effectively maintain the indoor thermal comfort and air quality.

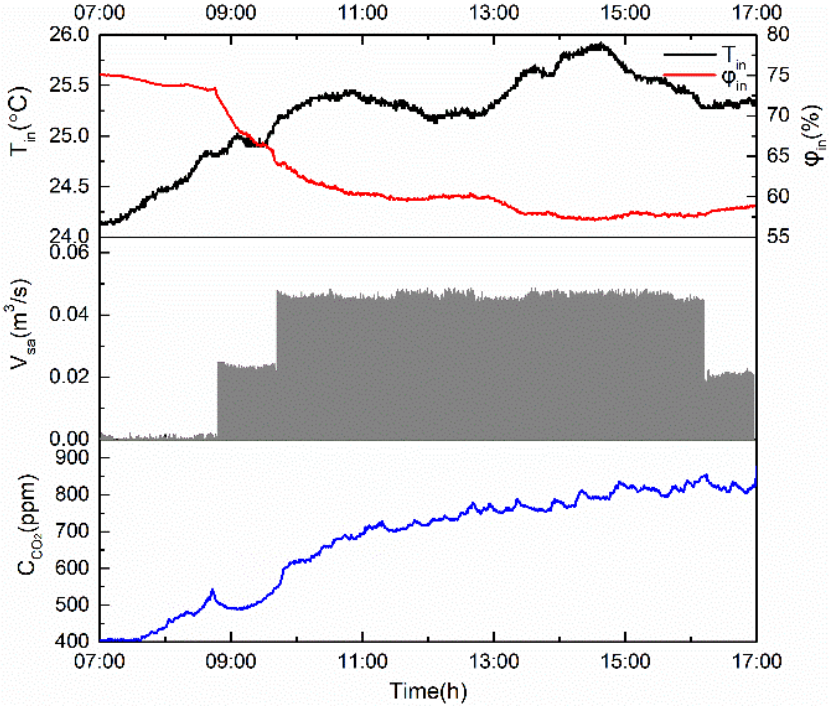

Fig. 16 The changes of T_{in}, φ_{in}, and C_{CO2} when V_{sa} is regulated based on the number of occupants.

3.4.2 Responses based on C_{CO2}

Based on the low initial φ_{in} on Sep. 2, the DV system was not started until the increases in occupants and equipment (ΔQ_{sen} = 344 W, ΔQ_{lat} = 146 W) caused C_{CO2} to reach nearly 700 ppm. The DV system operated at V_{sa_max} to remove the accumulated thermal and humidity loads in the room and dilute the C_{CO2}. Fig. 17 presents the changes of T_{in}, φ_{in}, and C_{CO2} when V_{sa} was regulated based on C_{CO2}. Upon initiation of the DV system, T_{in} continuously increased, while φ_{in} and C_{CO2} decreased significantly. The supply air flow rate was programed to decrease when the C_{CO2} was below 600 ppm, causing an obvious increase of the T_{in} and φ_{in}. When C_{CO2} approached 1000 ppm, the supply air flow rate was increased to V_{sa_max} to reduce the increased heat and humidity along with C_{CO2}. The DV system kept operating at V_{sa_max} after decreases in number of occupants to achieve further decreases in C_{CO2}. The supply air flow rate was greatly reduced half an hour after the three indoor air parameters had stabilized. Since the DV system responds quickly, it has the ability of effectively counteract changes in indoor thermal and humidity loads, and regulating the supply air flow rate based on C_{CO2} was effective at not only keeping T_{in}, φ_{in}, and C_{CO2} below the

required limits, but also reducing energy consumption.

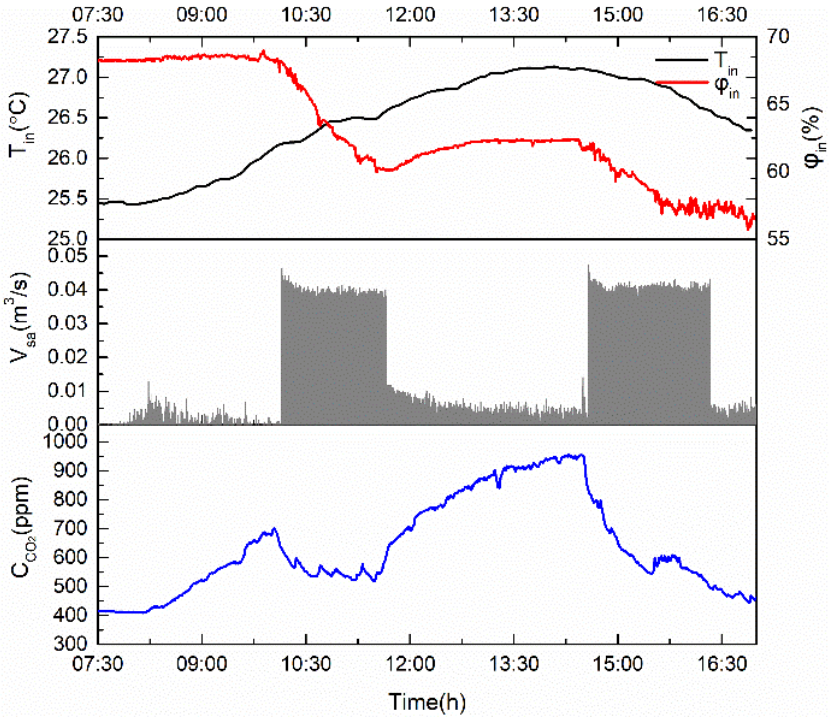

Fig. 17 The changes of T_{in}, φ_{in}, and C_{CO2} when V_{sa} was regulated based on C_{CO2}.

4 Discussion

The basic control method of the composite system was established in the beginning. Then the specific control strategies for an experimental room were proposed based on the basic control method to deal with typical cases including pre-dehumidification, intermittent operation, and sudden changes of indoor heat gain. For the case of pre-dehumidification using the air supply system, the most common approaches manipulate start-up times and supply air flow rate according to the cooling load characteristics in the numerical method [55]. Moreover, to maintain acceptable indoor air parameters and remove the latent heat load, a supplementary cooling strategy using air supply system is required. Therefore, this study conducted a field study to determine the pre-dehumidification time required for an air supply system on the basis of initial T_{in} and φ_{in} as well as changes in indoor heat gain. Then the parameters of V_{sa} and T_{sa} were regulated to ensure there was sufficient cooling for the indoor thermal environment. This method was proved more effective and practical as it was based on the outdoor weather condition and indoor heat gains changes in a real-world scenario.

In the case of intermittent operation control, it is crucial to analyze the thermal response performance of the radiant terminal which is characterized by τ_{63} and τ_{95}. The radiant terminal surface temperature is commonly selected as the characteristic parameter for RFC systems, and it is monitored by placing floor temperature sensors along the water flow direction (vertical) in the pipe of the radiant terminal and along the orientation of parallel pipes (horizontal) [56]. The decreasing gradient of surface temperature during intermittent operation was observed along with τ_{63} and τ_{95} to quantify the thermal response performance of the radiant terminal. Similarly, the floor temperature decay process and radiant uniformity were measured in this study. $\tau_{precooling}$ (τ_{95} = 2.5~3τ_{63}) during intermittent operation control was determined by analyzing the thermal response. This created a more realistic study that can provide practical suggestions for engineering

applications of radiant cooling systems.

In the case of sudden changes of indoor heat gain, the operational performance of RFC combined DV systems is estimated by monitoring T_{in} distribution and ventilation efficiency [37]. This study took the indoor environment parameter as the first target for adjusting the supply air flow rate and temperature due to the slower thermal response of radiant floor systems. Meanwhile, thermal comfort was continuously evaluated to achieve the optimal control of the radiant cooling system. In summary, compared to similar studies, the unique advantage of this study was that it accounted for real-world weather conditions and indoor environmental changes and was able to demonstrate the abilities of different control strategies in an effective and practical way.

However, the present study only focused on the operational control of an RFC system composed of one fixed material type and DV system, so experimental results may be different if other materials are used. Phase change material (PCM) is a common material used in radiant systems. Compared with conventional concrete materials, PCM can maintain small temperature differences between internal surfaces and indoor air temperature, reducing temperature fluctuations and decreasing the peak load due to its high latent heat storage capacity . It has been shown that, compared to conventional radiant cooling panels, macro-encapsulated PCM panels improved operational flexibility of radiant systems by shifting the entire cooling load to off-peak hours [57]. Moreover, the thermal energy stored in PCM radiant floors is higher compared to classical concrete radiant floors, and solidification rates of PCM depend mainly on the indoor air temperature and cover thickness [58]. It was also noted that heat released by double-layer PCM during its solidification can slow the temperature increase of the floor surface and increase the cold energy stored by the radiant floor system in summer [59]. Therefore, the interactions between seasonal factors and different materials and the correlations between various materials and indoor temperature and humidity should also be considered to provide a more comprehensive conclusion.

There were also some limitations related to the experimental conditions. It was not feasible to achieve individual room control via independently regulating supply air temperature due to the unified control mode of the air systems in the building, which revealed inflexibility operational control of composite system in the fixed experimental scenario. As a result, the control method of composite system cannot be sufficiently utilized so that showing unobvious application value.

Consequently, it is necessary to conduct further studies on operational control correlative to the thermal performance of radiant systems composed of different materials and make modification on the basis of the study to achieve more reliable control for different material types. In addition, more effort should be made to study independent and personal control of cooling systems through the automated control technology in the future, e.g., using model predictive controls[60], and unknown-but-bounded[61]. Derived from the automated control concept, it is necessary to figure out the physical characteristics of the building relevant to dynamic thermal behavior first. Then the operational control for heating / cooling are determined based on certain constraints (e.g. condensation on radiant surfaces) and uncertain disturbances (internal and external heat gains) to maintain the indoor environmental parameters inside the acceptable range[62]. Thus the future work will conduct the automated control on indoor thermal environment in the self-building test house. More accurate control will be applied to handle indoor load in the activation stage and counter the dynamic change of indoor heat gain in the operation stage so as to better prove the generality and feasibility of the control method. The ultimate objective is to achieve more advanced and practical control and provide reliable reference for the operational

control of composite system.

5 Conclusion

Based on the outdoor weather conditions and the indoor loads to be handled, the operational parameters of the DGCS with RFC and DV systems were regulated so that the cooling capacity matched the indoor cooling demand to keep the indoor temperature and humidity within their allowable ranges and ensure T_{op} remains within 26~27°C.

RFC control in this study included two intermittent operation strategies. For the scenario using intermittent operation on weekends, precooling began 2.5~3 times τ_{63} before work time in order to enable the systems cooling capacity to meet the cooling requirements. In the scenario using intermittent operation at night on weekdays, the RFC supply water flow rate at night was reduced to 80% of that during the working period, which was determined based on the indoor cooling requirement. It was critical that both strategies ensure sufficient cooling so that the floor surface temperature during working periods was within the acceptable range.

The DV system was controlled in two ways. The first was based on the variable initial temperature and humidity conditions in the room. When $\varphi_{in} > 75\%$ and $T_{in} > 26$°C, the DV system was started 1~1.5 h before the work time as required by the latent heat load to be removed and the dehumidification rate. In this case the supply water flow rate was maintained at V_{sa_max}. When $\varphi_{in} > 75\%$ and $T_{in} < 26$°C, the DV system was started at V_{sa_max} for dehumidification and then the supply air flow rate was regulated so as to counteract indoor heat gain. When $\varphi_{in} < 75\%$ and $T_{in} < 26$°C, the start-up time of DV system was initiated when cooling capacity of the RFC system was insufficient, and the supply air temperature was increased by 1~2°C at the initial time. Moreover, the outdoor air was used for indoor ventilation when $T_{out} \leq 28$°C and $\varphi_{out} \leq 70\%$ that were suitable for the comfort requirements.

The second DV system control was set to respond to sudden increases in indoor heat gain (ΔQ_{sen} = 344W, ΔQ_{lat} = 146W). The supply air flow rate operated at 50% V_{sa_max} at first for dehumidification ($\varphi_{in} > 70\%$ and $T_{in} < 26$°C) and increased to V_{sa_max} to counter sudden increases in indoor heat gain. Moreover, the DV system was not activated at low indoor loads ($\varphi_{in} < 70\%$ and $T_{in} < 26$°C), and was only started when sudden increases in occupants caused the C_{CO2} to increase to a high level. The supply air flow rate was initially set at V_{sa_max}, but then regulated based on the changes of indoor thermal environment parameters.

This study proposed control methods for a combined RFC and DV system. The control methods had positive effects on the indoor comfort as well as the energy savings of the cooling system, and with further study more accurate control can be achieved to optimize performance.

Acknowledgements

This work was funded by the Support Plan for Outstanding Youth Innovation Team in Colleges and Universities of Shandong Province (2019KJG005) and National Natural Science Foundation of Shandong Province (ZR2020ME211). This work was also supported by the Plan of Introduction and Cultivation for Young Innovative Talents in Colleges and Universities of Shandong Province.

Nomenclature

NV	natural ventilation
Q	indoor heat gain (W)
Q'	system cooling capacity (W)

S	radiant uniformity coefficient
S_n	measured point
T	temperature (℃)
$T_{0.1}$	indoor air temperature at the vertical height of 0.1 m (℃)
T_{dp}	indoor air dew point temperature (℃)
T_{f_nol}	floor surface temperature under normal operation (℃)
T_{max}	limited highest indoor air temperature, 28℃
T_{mrt}	mean radiant temperature (℃)
T_{op}	operative temperature (℃)
T_{out}	outdoor air temperature
V	volume flow rate (m^3/s)
V_{sa_max}	supply air flow rate when the air inlets are all open (m^3/s)
V_{sw_max}	maximum supply water flow rate (m^3/s)
W	dehumidification amount to be removed (g/h)
W'	dehumidification capacity (g/h)

Subscripts

in	indoor air
f	floor surface
out	outdoor air
sa	supply air
sw	supply water
rw	return water
sen,	indoor sensible heat gain
lat	indoor latent heat gain

Symbols

τ	time from current time to start time of work (h)
τ_{63}	time to achieve 63% of the temperature change (h)
τ_{final}	time to achieve the whole temperature change (h)
$\tau_{precooling}$	Precooling time of RFC (h)
φ_{in}	indoor air relative humidity (%)
φ_{max}	limited highest indoor relative humidity, 70%
φ_{out}	outdoor air relative humidity (%)
ω	humidity ratio (g/kg)

Appendix A. Theoretical basis for control strategies

The control method and technology route of the study is shown in Fig. A1. The operation of RFC system and DV system were regulated in response to the outdoor weather condition and indoor heat gains in the real-world scenario, along with actual and reliable control effect reflected by the changes of indoor thermal environment parameter. The explanation of control strategies for three typical cases obtained from the experimental test are illustrated as follow.

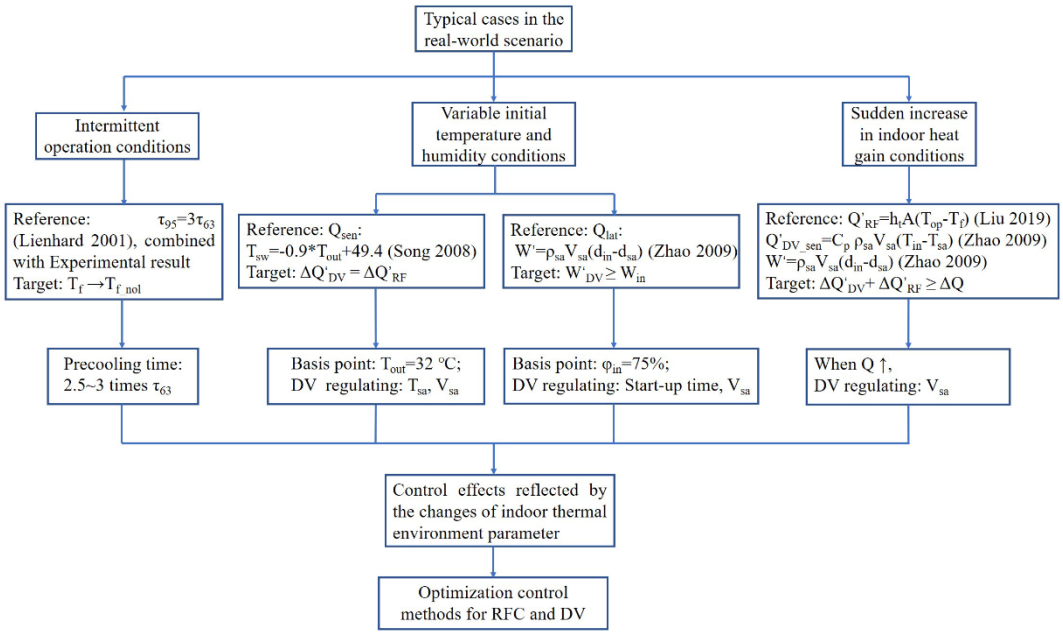

Fig. A1 The control method and technology route of this study.

(1) In the case of the intermittent condition, the theoretical τ_{63} of radiant panel in the experiment is 5.1 h without considering the short wave radiation calculated by Eq. (A.1) [48], but the experimental τ_{63} was greater than the theoretical τ_{63} due to the influence of solar radiation in the real-world scenario.

$$\tau_{63} = \frac{C}{1/R+h_c+h_r} \quad (A.1)$$

where, C is equivalent heat capacity of radiant panel, kJ/(m^2·K); R is thermal resistance, (m^2·K)/W; h_c is convection heat transfer coefficient, W/(m^2·K); and h_r is the radiation heat transfer coefficient, W/(m^2·K). For this experiment, the above parameters were defined as: C = 247.4 kJ/(m^2·K), R = 0.154 (m^2·K)/W, h_c = 1.5 W/(m^2·K), and h_r = 5.5 W/(m^2·K).

According to the study by Lienhard [49], the response time τ_{95} is generally three times τ_{63}. Considering the thermal response of the radiant floor in this field experiment, $\tau_{precooling}$ required for RFC system was finally determined as 2.5~3 times of τ_{63}.

(2) In the case of variable initial temperature and humidity conditions in the room, the control methods for handling indoor sensible heat load were obtained according to the correlation between supply water temperature and outdoor air temperature. The empirical equation is shown in Eq. (A.2) [50].

$$T_{sw} = -0.9T_{out} + 49.4 \quad (A.2)$$

where, the T_{sw} is the underground circulating water temperature in this study. During the measurement, T_{sw} of RFC system varied from 20 to 20.5°C. The maximum T_{sw} of 20.5°C was selected in the equation and T_{out} was obtained as approximately 32°C, which meant that when T_{out} reached 32°C, the required T_{sw} was 20.5 °C. Therefore, the key point of outdoor air temperature is determined as 32°C to adjust the operational parameters of DV and RFC system. However, T_{sw} of the RFC system could not be regulated and V_{sw} regulation had little effect on indoor thermal environment. As a result, it was required that the change of the cooling capacity via regulating supply air parameters be the same as that via the regulation of T_{sw} in the RFC system, achieving a matching control effect.

Moreover, the control methods for handling indoor latent heat load were as follows. The designed supply air parameter of the DV system in the experimental study was 24℃ and 55%, and T_{in} and φ_{in} of the experimental room were required to be 26℃ and 65% by the work time (9:00). Therefore, the dehumidification capacity of the DV system was calculated to be 805.73 g/h by taking the above parameters into Eq. (A.3) [63].

$$W' = \rho_{sa} V_{sa} (d_{in} - d_{sa}) \quad \text{(A.3)}$$

where, ρ_{sa} is density of supply air, kg/m^3; d_{in} is humidity ratio of indoor air, g/kg; and d_{sa} is humidity ratio of supply air, g/kg.

During the experimental test, the highest initial T_{in} was 27℃ before the normal start-up time (8:00) of the DV system. When the initial T_{in} and φ_{in} were 27°C and 75% and were required to decrease to 26°C and 65% by 9:00, the target indoor dehumidification amount was 794.9 g/h. Based on the dehumidification capacity (805.73 g/h) of the DV system, the pre-dehumidification time should be 1 h. Accordingly, the DV system was supposed to be initiated at 8:00 which was the normal start-up time. The air humidity (75%) was taken as the threshold to determine the start-up time and V_{sa} of the DV system and change the dehumidification capacity in the face of indoor latent heat load to be removed and control φ_{in} to meet the design requirements.

(3) In the case of sudden increases in indoor heat gain condition (ΔQ_{sen} = 344W, ΔQ_{lat} = 218 g/h), based on the control requirements included the increase of T_{in} within 1°C along with no increase in φ_{in}, V_{sa} was increased by 50%.

The sensible heat load burdened by RFC system is calculated by Eq (A.4) [48].

$$Q'_{RF} = h_t A (T_{op} - T_f) \quad \text{(A.4)}$$

where, h_t is total heat transfer coefficient, W/(m^2·K); A is experimental room area, m^2; T_{op} is operative temperature, °C; and T_f is floor surface temperature, °C.

The sensible heat load burdened by DV system is calculated by Eq (A.5) [63].

$$Q'_{DV\_sen} = C_p \rho_{sa} V_{sa} (T_{in} - T_{sa}) \quad \text{(A.5)}$$

where, C_p is specific heat of supply air, J/(kg·°C); ρ_{sa} is density of supply air, kg/m^3; V_{sa} is supply air volume flow rate, m^3/s; T_{in} is indoor temperature, °C; and T_{sa} is supply air temperature, °C.

Compared with cooling performance of the composite system before implementing control, the total cooling capacity of the RFC system and DV system calculated by Eq (A.3) and Eq (A.4) was increased by 366 W, and the dehumidification capacity of the DV system calculated by Eq. (A.3) was increased by 231 g/h by utilizing control strategies. Therefore, the improved dehumidification capacity was sufficient to remove the excessive heat and humidity load caused by the sudden increase of indoor heat source and achieve the control requirements.

In conclusion, these optimized control methods for the three typical cases supported by precise scientific basis had prospective effect on indoor thermal environment, which indicated that control strategies were reliable and applicable so that providing a trustworthy reference for optimal operation of the composite system in practical application.

References

[1] Rhee K-N, Kim K W. A 50 year review of basic and applied research in radiant heating and cooling systems for the built environment[J]. Building and Environment, 2015, 91: 166-190.

[2] Yang B, Ding X, Wang F, et al. A review of intensified conditioning of personal micro-environments: Moving closer to the human body[J]. Energy and Built Environment, 2021, 2(3): 260-270.

[3] Kim M K, Liu J, Cao S-J. Energy analysis of a hybrid radiant cooling system under hot and humid climates: A case study at Shanghai in China[J]. Building and Environment, 2018, 137: 208-214.
[4] Liu J, Li Z, Kim M K, et al. A comparison of the thermal comfort performances of a radiation floor cooling system when combined with a range of ventilation systems[J]. Indoor and Built Environment, 2020, 29(4): 527-542.
[5] Tian Z, Love J A. A field study of occupant thermal comfort and thermal environments with radiant slab cooling[J]. Building and Environment, 2008, 43(10): 1658-1670.
[6] Babiak J, Olesen B W, Petras D. Low Temperature Heating and High Temperature Cooling-System Types and Estimation of Heating/Cooling Capacity[J]. REHVA Journal, 2007, 44(3).
[7] Kazanci O. Low Temperature Heating and High Temperature Cooling in Buildings[D]. Technical University of Denmark, 2016.
[8] Bojić M, Cvetković D, Marjanović V, et al. Performances of low temperature radiant heating systems[J]. Energy and Buildings, 2013, 61: 233-238.
[9] Sevilla L T, Radulovic J. Investigation of low grade thermal energy storage systems with phase changing materials[J]. Energy and Built Environment, 2021, 2(4): 366-373.
[10] Liu X, Yi X, Xie X, et al. Temperature and humidity independent control air-conditioning system and operating strategy[C]. The 22nd International Congress of Refrigeration, 2007.
[11] Andrés-Chicote M, Tejero-González A, Velasco-Gómez E, et al. Experimental study on the cooling capacity of a radiant cooled ceiling system[J]. Energy and Buildings, 2012, 54: 207-214.
[12] Liu J, Kim M K, Srebric J. Numerical analysis of cooling potential and indoor thermal comfort with a novel hybrid radiant cooling system in hot and humid climates[J]. Indoor and Built Environment, 2021: 1420326X211040853.
[13] Bauman F, Feng J D, Schiavon S. Cooling load calculations for radiant systems: are they the same traditional methods?[J]. Ashrae Journal, 2013, 55(12): 20-27.
[14] Zhang C, Pomianowski M, Heiselberg P K, et al. A review of integrated radiant heating/cooling with ventilation systems- Thermal comfort and indoor air quality[J]. Energy and Buildings, 2020, 223: 110094.
[15] Song D, Kim T, Song S, et al. Performance evaluation of a radiant floor cooling system integrated with dehumidified ventilation[J]. Applied Thermal Engineering, 2008, 28(11-12): 1299-1311.
[16] Krajčík M, Šikula O. The possibilities and limitations of using radiant wall cooling in new and retrofitted existing buildings[J]. Applied Thermal Engineering, 2020, 164: 114490.
[17] Ning B, Schiavon S, Bauman F S. A novel classification scheme for design and control of radiant system based on thermal response time[J]. Energy and Buildings, 2017, 137: 38-45.
[18] Jin W, Jia L, Wang Q, et al. Study on Condensation Features of Radiant Cooling Ceiling[J]. Procedia Engineering, 2015, 121: 1682-1688.
[19] Mohannad B.. Method to Integrate Radiant Cooling with Hybrid Ventilation to Improve Energy Efficiency and Avoid Condensation in Hot, Humid Environments[J]. Buildings, 2018, 8(5): 69.
[20] Chen X, Riffat S, Bai H, et al. Recent progress in liquid desiccant dehumidification and air-conditioning: A review[J]. Energy and Built Environment, 2020, 1(1): 106-130.
[21] Wang Y, Yin Y, Zhang X, et al. Study of an integrated radiant heating/cooling system with fresh air supply for household utilization[J]. Building and Environment, 2019, 165: 106404.
[22] Rhee K-N, Olesen B W, Kim K W. Ten questions about radiant heating and cooling systems[J]. Building and Environment, 2017, 112: 367-381.
[23] Liu J, Zhu X, Kim M K, et al. A Transient Two-dimensional CFD Evaluation of Indoor Thermal

Comfort with an Intermittently-operated Radiant Floor Heating System in an Office Building[J]. International Journal of Architectural Engineering Technology, 2020, 7: 62-87.
[24] Hu R, Niu J L. Operation dynamics of building with radiant cooling system based on Beijing weather[J]. Energy and Buildings, 2017, 151: 344-357.
[25] Wu W. Low-temperature compression-assisted absorption thermal energy storage using ionic liquids[J]. Energy and Built Environment, 2020, 1(2): 139-148.
[26] Khan R J, Bhuiyan M Z H, Ahmed D H. Investigation of heat transfer of a building wall in the presence of phase change material (PCM)[J]. Energy and Built Environment, 2020, 1(2): 199-206.
[27] Cho S H, Zaheer-Uddin M. Predictive control of intermittently operated radiant floor heating systems[J]. Energy Conversion and Management, 2003, 44(8): 1333-1342.
[28] Sui X, Wang H, Yan J, et al. Optimal Intermittent Regulation of Tubes-embedded Building Envelope Cooling System[J]. Procedia Engineering, 2017, 205: 2639-2646.
[29] Zhang L, Liu J, Heidarinejad M, et al. A Two-Dimensional Numerical Analysis for Thermal Performance of an Intermittently Operated Radiant Floor Heating System in a Transient External Climatic Condition[J]. Heat Transfer Engineering, 2020, 41(9-10): 825-839.
[30] Lim J H, Jo J H, Kim Y Y, et al. Application of the control methods for radiant floor cooling system in residential buildings[J], 2006, 41(1): 60-73.
[31] Tang H, Raftery P, Liu X, et al. Performance analysis of pulsed flow control method for radiant slab system[J]. Building and Environment, 2018, 127: 107-119.
[32] Liu J, Dalgo D A, Zhu S, et al. Performance analysis of a ductless personalized ventilation combined with radiant floor cooling system and displacement ventilation[J]. Building Simulation, 2019, 12(5): 905-919.
[33] Liu J, Zhu S, Kim M K, et al. A Review of CFD Analysis Methods for Personalized Ventilation (PV) in Indoor Built Environments[J]. Sustainability, 2019, 11(15).
[34] Causone F, Corgnati S P, Filippi M, et al. Experimental evaluation of heat transfer coefficients between radiant ceiling and room[J]. Energy and Buildings, 2009, 41(6): 622-628.
[35] Shan W, Rim D. Thermal and ventilation performance of combined passive chilled beam and displacement ventilation systems[J]. Energy and Buildings, 2018, 158: 466-475.
[36] Yu T, Heiselberg P, Lei B, et al. A novel system solution for cooling and ventilation in office buildings: A review of applied technologies and a case study[J]. Energy and Buildings, 2015, 90: 142-155.
[37] Krajčík M, Tomasi R, Simone A, et al. Thermal comfort and ventilation effectiveness in an office room with radiant floor cooling and displacement ventilation[J]. Science and Technology for the Built Environment, 2015, 22(3): 317-327.
[38] Cui S, Kim M K, Papadikis K. Performance Evaluation of Hybrid Radiant Cooling System Integrated with Decentralized Ventilation System in Hot and Humid Climates[J]. Procedia Engineering, 2017, 205: 1245-1252.
[39] Arghand T, Javed S, Trüschel A, et al. Cooling of office buildings in cold climates using direct ground-coupled active chilled beams[J]. Renewable Energy, 2021, 164: 122-132.
[40] Li Z, Zheng M. Development of a numerical model for the simulation of vertical U-tube ground heat exchangers[J]. Applied Thermal Engineering, 2009, 29(5-6): 920-924.
[41] Arghand T, Javed S, Trüschel A, et al. Control methods for a direct-ground cooling system: An experimental study on office cooling with ground-coupled ceiling cooling panels[J]. Energy and Buildings, 2019, 197: 47-56.

[42] Liu L, Yu Z, Zhang H, et al. Performance improvements of a ground sink direct cooling system under intermittent operations[J]. Energy and Buildings, 2016, 116: 403-410.
[43] Romaní J, Pérez G, De Gracia A. Experimental evaluation of a cooling radiant wall coupled to a ground heat exchanger[J]. Energy and Buildings, 2016, 129: 484-490.
[44] Krajčík M, Šikula O. Heat storage efficiency and effective thermal output: Indicators of thermal response and output of radiant heating and cooling systems[J]. Energy and Buildings, 2020, 229: 110524.
[45] Jin W, Jing J, Jia L, et al. The dynamic effect of supply water flow regulation on surface temperature changes of radiant ceiling panel for cooling operation[J]. Sustainable Cities and Society, 2020, 52: 101765.
[46] Shin M S, Rhee K N, Ryu S R, et al. Design of radiant floor heating panel in view of floor surface temperatures[J]. Building and Environment, 2015, 92: 559-577.
[47] Annual Report on China Building Energy Efficiency[M]. China Architecture & Building Press, 2014.
[48] Liu X, Zhang T, Zhou X, et al. Radiant Cooling[M]. China Architecture & Building Press, 2019.
[49] Lienhard Iv J H, Lienhard V J H. A Heat Transfer Textbook (third edition)[M]. Phlogiston Press Cambrige, Massachusetts, U .S .A, 2006.
[50] Song D, Kim T, Song S, et al. Performance evaluation of a radiant floor cooling system integrated with dehumidified ventilation[J]. Applied Thermal Engineering, 2008, 28(11): 1299-1311.
[51] Liu J, Xie X, Qin F, et al. A case study of ground source direct cooling system integrated with water storage tank system[J]. Building Simulation, 2016, 9(6): 659-668.
[52] Feng J, Schiavon S, Bauman F. Cooling load differences between radiant and air systems[J]. Energy and Buildings, 2013, 65: 310-321.
[53] Liu J, Ren J, Zhang L, et al. Optimization of Control Strategies for the Radiant Floor Cooling System Combined with Displacement Ventilation: A Case study of an Office Building in Jinan, China[J]. International Journal of Architectural Engineering Technology, 2019, 6: 33-48.
[54] Ashrae Standard 55. Thermal environmental Conditions for Human Occupancy, American Society of Heating, Refrigerating and Air-Conditioning Engineers[R]. Atlanta, USA, 2004.
[55] Lim J-H, Song J-H, Song S-Y. Development of operational guidelines for thermally activated building system according to heating and cooling load characteristics[J]. Applied Energy, 2014, 126: 123-135.
[56] Sun H, Wu Y, Lin B, et al. Experimental investigation on the thermal performance of a novel radiant heating and cooling terminal integrated with a flat heat pipe[J]. Energy and Buildings, 2020, 208: 109646.
[57] Bogatu D-I, Kazanci O B, Olesen B W. An experimental study of the active cooling performance of a novel radiant ceiling panel containing phase change material (PCM)[J]. Energy and Buildings, 2021, 243: 110981.
[58] González B, Prieto M M. Radiant heating floors with PCM bands for thermal energy storage: A numerical analysis[J]. International Journal of Thermal Sciences, 2021, 162: 106803.
[59] Sun W, Zhang Y, Ling Z, et al. Experimental investigation on the thermal performance of double-layer PCM radiant floor system containing two types of inorganic composite PCMs[J]. Energy and Buildings, 2020, 211: 109806.
[60] Joe J, Karava P. A model predictive control strategy to optimize the performance of radiant floor heating and cooling systems in office buildings[J]. Applied Energy, 2019, 245: 65-77.

[61] Gwerder M, Lehmann B, Tödtli J, et al. Control of thermally-activated building systems (TABS)[J]. Applied Energy, 2008, 85(7): 565-581.
[62] Romaní J, De Gracia A, Cabeza L F. Simulation and control of thermally activated building systems (TABS)[J]. Energy and Buildings, 2016, 127: 22-42.
[63] Zhao R, Fan C, Xue D, et al. Air Conditioning[M]. China Architecture & Building Press, 2009.